



# Soil Salinity, Agriculture, and Nature Conservation in Monegros, NE Spain

**M. Tierra<sup>1</sup>, C. Castañeda<sup>1\*</sup>, F. J. Gracia<sup>2</sup> and E. T. Medina<sup>1</sup>**

<sup>1</sup>Estación Experimental de Aula Dei, EEA-CEA-CSIC, Zaragoza, Spain, <sup>2</sup>Department Earth Sciences, Faculty of Marine and Environmental Sciences, University of Cádiz, Cádiz, Spain

Salinity is a determining factor for agriculture due to its effects on crops. The Common Agricultural Policy (CAP) of European Union does not take this concept into account when distributing monetary aid to farmers. The Central Ebro Basin (CEB) presents this problem due to the semiarid climate conditions and the composition of the soils, generating an economic suffocation in the rural areas of the region. The present work aims to evaluate salinity in a dry-farmed landscape surrounding the “Saladas of Sástago-Bujaraloz,” a protected area under agricultural intensification with extreme saline conditions. We analyzed the saline composition of the soil of three saladas along transects and we surveyed the soil salinity with electromagnetic sensor (EMS) to facilitate the inspection of salinity in the field. The electrical conductivity (EC) ranged from slightly saline to very strongly saline. A 73% of the 319 soil samples analysed were very strongly saline ( $EC_e > 16 \text{ dS m}^{-1}$ ) and half of the very strongly saline soil samples were taken in crop areas. The mean  $EC_{1:5}$  varied from  $15 \text{ dS m}^{-1}$  in the saladas to a range of  $3-4.6 \text{ dS m}^{-1}$  in the crops. There was a noticeable variability of the vertical distribution of soil salinity and a high salinity range in the upper soil horizons of natural areas. In general, the salinity of the integrated 100 cm of soil depth ( $EC_{e100}$ ) was higher than that of 50 cm ( $EC_{e50}$ ). The correlation between the EMS readings and EC varied between saladas, between horizontal and vertical readings, and between integrated soil depths. The best relationship was found with a soil depth of 0–100 cm and with horizontal EMS readings. The identified salinity patterns are consistent and applicable in the whole area of about 150 saladas. The purpose is to suggest salinity as an agronomic criterion within the CAP regulations. A proposed new agri-environment-climate measure could include classifying plots with  $EC_e > 10 \text{ dS m}^{-1}$  in more than 50% of the area as unsuitable for cultivation.

## OPEN ACCESS

### Edited by:

Alberto Enrique,  
Public University of Navarre, Spain

### \*Correspondence

C. Castañeda,  
ccastaneda@eead.csic.es

**Received:** 31 July 2025

**Revised:** 03 December 2025

**Accepted:** 11 December 2025

**Published:** 07 January 2026

### Citation:

Tierra M, Castañeda C, Gracia FJ and Medina ET (2026) Soil Salinity, Agriculture, and Nature Conservation in Monegros, NE Spain. *Span. J. Soil Sci.* 15:15359. doi: 10.3389/sjss.2025.15359

## INTRODUCTION

Both in arid or semiarid inland regions and in coastal areas, soil salinity—whether natural or induced by human activities—occurs worldwide, as is the case in the Mediterranean region. Salinity threatens agriculture but, on the other hand, saline areas harbor organisms whose rarity and adapted metabolism give them a high scientific and social value. Therefore, knowing the distribution of soil salinity in the landscape is crucial not only for crop management and the protection of saline ecosystems, but also for the sustainability of agriculture.

Spain contains the largest surface of saline land in the European Union (Tóth et al., 2008; FAO, 2024). Traditionally, the saline areas supported low-income rainfed farming and extensive livestock

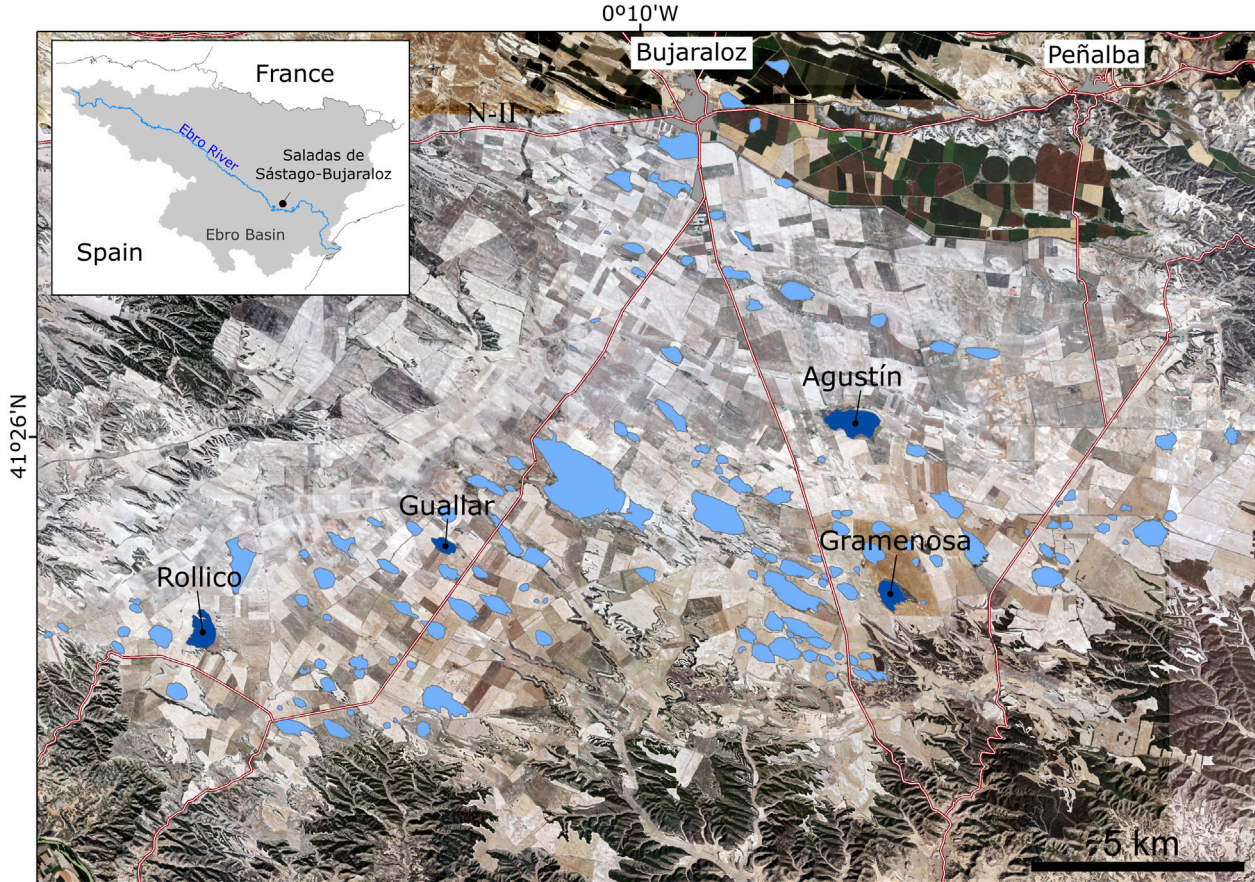


**FIGURE 1** | Distribution of the saladas of Sástago-Bujaraloz in the dryfarmed area of Monegros. At the top of the PNOA background image, the irrigated area with the towns indicated. The four wetlands studied in this work are in dark blue and labelled.

activities, with minor impacts on the environment. In this scenario, the hypersaline wetlands—now protected by environmental legislation—were conserved. This is the case of our study area (Figure 1), the Monegros region located in the central Ebro Basin (CEB).

Over the last decades, Monegros has undergone radical transformations with strong impacts on its ecological functions affecting the survival of the saline enclaves (Pedrocchi and Sanz, 1991; Domínguez-Beisiegel et al., 2013a). These transformations include irrigation schemes both in operation and in progress, or intensive swine farms that are legally spreading slurry causing an excess of 441 t N in the basin (Tierra et al., 2025). Upcoming transformations include electricity production by solar panels and windmills, whose effects on near-surface wind speed, ground temperature and evaporation remain poorly known.

The Saladas of Sástago-Bujaraloz in Monegros are saline wetlands with alternating inundation and drying episodes and with a water salinity in some of their bottoms 10 times higher than that of the sea water. Their water regime, together with their chemical characteristics and semiarid climate (Herrero and Snyder, 1997), make possible a unique vegetation, unparalleled

in Europe (Conesa et al., 2011; FAO, 2024). These closed depressions scattered in the landscape were surrounded by rainfed winter cereals—mainly barley (*Hordeum vulgare* L.)—as far as the topography and the soil salinity allow, and often with crops sowed even within the wetland depressions. Yields, controlled by the scarce and variable seasonal rainfall, are very irregular (McAneney and Arrué, 1993; Castañeda and Moret-Fernández, 2013). The socioeconomic scenario was modified by European Union subsidies and the prospects of conversion to irrigation. Protected saline habitats are sensitive to land use changes at the wetland-crop interface and could be affected by agricultural actions, in some cases with the main objective of earning subsidies. The protection of saladas ought to consider the extent and variability of salinity not only in their bottoms, but also in surrounding agricultural soils.

Since the later 20th century, field assessment and mapping of a number of soil characteristics have become affordable in terms of cost and time thanks to the advent of portable electromagnetic sensor (EMS) (McNeill, 1991). Soil salinity appraisal using EMS is a well-established technique used in many countries (Corwin and Scudiero, 2019) including the CEB, e.g., Herrero and Pérez-Coveta (2005) or Casterad et al. (2018), illustrating how the

EMS-directed sampling reduces the number of soil samples needed.

The objective of this work is to implement edaphic salinity as a criterion to regulate agricultural activity by establishing limits for cultivation in the wetland-crop interface, without affecting the farmer's subsidies. With this purpose, we studied usefulness of the EMS in relation to the geomorphological setting in order to speed up the field survey and to reduce the number of soil samples needed.

## STUDY AREA

A complex of almost 150 playa-lakes and closed depressions hosting temporary saline wetlands occurs in three conterminous municipalities, Sástago, Peñalba and Bujaraloz, located in the CEB (Figure 1). The Saladas of Sástago-Bujaraloz belong to the European Natura 2000 network of protected areas (ES2430082 and ES0000181) and to the Ramsar list of wetlands of international importance (Ramsar Convention Secretariat, 2010). These wetlands, with elevations ranging from 320 m to 417 m a.s.l., occupy depressions of karstic and aeolian origin developed on subhorizontal continental Tertiary limestones intercalated with gypsum and saliferous lutites (Salvany et al., 1996).

The climate is characterized by interannual and seasonal irregular scarce rains, high temperature fluctuations and a persistent NW dry wind. These factors result in high hydric deficit in the area. Daily data from the nearby Valfarta weather station (SIAR network<sup>1</sup>) give an annual mean precipitation of 358.8 mm, 1,261.7 mm of evapotranspiration ( $ET_0$ ), and a temperature of 14.1 °C for the period 2004–2024. Despite the hydric deficit, most saline wetlands maintain a wet bottom and a sheet of water with variable persistence (Castañeda et al., 2005) due to the groundwater supply, which reach 40% of the total water input into the wetlands (Castañeda and García-Vera, 2008). Groundwater is highly saline reaching 175 dS m<sup>-1</sup> (Paracuellos, 2006).

Soil development is conditioned by the climate and the lithology. The salinity of the soils is related to the saliferous lutites, main source of the groundwater salinity. The agricultural area surrounding the saladas has non-saline soils rich in carbonate and gypsum with low organic matter content (Castañeda et al., 2009). The saladas bottoms are extremely flat and are very saline with the formation of salt crust (Domínguez-Beisiegel et al., 2013b). Deep plowing with breakage of limestone and gypsum strata and their removal causes crop roots to gain access to saline materials (Cuchí, 1986).

Farmers have been demanding for decades the conversion of the area into irrigation. Several authors have indicated that this would lead to a rise in the shallow phreatic level due to the occurrence of perched groundwater levels and a low permeability of the geological materials (Cuchí, 1986; García-Vera, 1996; Castañeda, 2002). A decrease in arable land due to flooding

and soil salinization can be expected. We selected four of the nearly 150 wetlands inventoried in the area by Castañeda et al. (2013) for study. The names of the selected saladas are Agustín, Gramenosa, Guallar and Rollico (Figure 1).

## MATERIALS AND METHODS

### Geomorphological Mapping

A detailed geomorphological map of the studied wetlands was made through stereoscopic photointerpretation of contacts at 1:33000 scale of the aerial photographs of USAF-B flight (1956–1957). The photointerpretation was digitalized and georeferenced using the geographic information system ArcGIS<sup>®</sup> (v.10.8.2). The topography of the wetlands basins was analysed by using a digital elevation model (DEM) with a pixel of 2 m derived from LiDAR-PNOA-cob2 2015 CC-BY 4.0 (scne.es) with a density of 0.5 point per m<sup>-2</sup>.

### Soil Survey Strategy

Four of the largest saladas were selected as representative of the diverse wetland types recognized in the endorheic system (Castañeda et al., 2013): the playa lakes Rollico (40.8 ha) and Guallar (14.9 ha) with bare bottom, and the wet basins Gramenosa (29.9 ha) and Agustín (62.5 ha) with perennial halophytes and arable land. All them are affected by advancing plowing and cropping as the soil wetness allows the machinery to enter. Agustín occupies the bottom of a flat-bottomed valley with a relatively smooth topography and a higher agriculture imprint.

Two different methods were used for the soil salinity survey. A first campaign consisted in soil sampling along transects extending through the wetland-crop interface. The transects include the bottom (bare or vegetated), fringe of natural vegetation, and agricultural plots. According to the basin geomorphology, these transects were of NW-SE direction in Guallar and Rollico, and of NE-SW direction in Gramenosa (Figures 2a–c). The second soil sampling campaign was conducted in Agustín, in agricultural plots declared as “arable land” in the Land Parcel Identification System (LPIS), the information system recording all agricultural parcels in the EU Member States and key control mechanism under the Common Agricultural Policy (CAP) (European Court of Auditors, 2016). The accessible fringing area of the wetland was sampled with the EM sensor and three of these surveyed plots, named A1, A2, and A3, were selected for soil sampling (Figure 2d). Table 1 summarizes the soil sampling characteristics. A total of 34 sites were sampled along the 1870 m of the three transects and 28 sites were distributed in three plots of Agustín over a total of 34.4 ha.

### Field Sampling

Soil samples were extracted by using a 7 cm diameter Eijkelkamp hand auger at 20 or 25 cm intervals. At the different sites, the sampling depth and/or the depth intervals were not the same (Table 1) due to their different surveys or operators. The sampled depth of the soil ranged from 50 to 260 cm. A total of 183 soil samples were taken along the transects and 136 distributed in agricultural plots, totaling 319 soil samples.

<sup>1</sup><https://servicio.mapa.gob.es/websiar/>

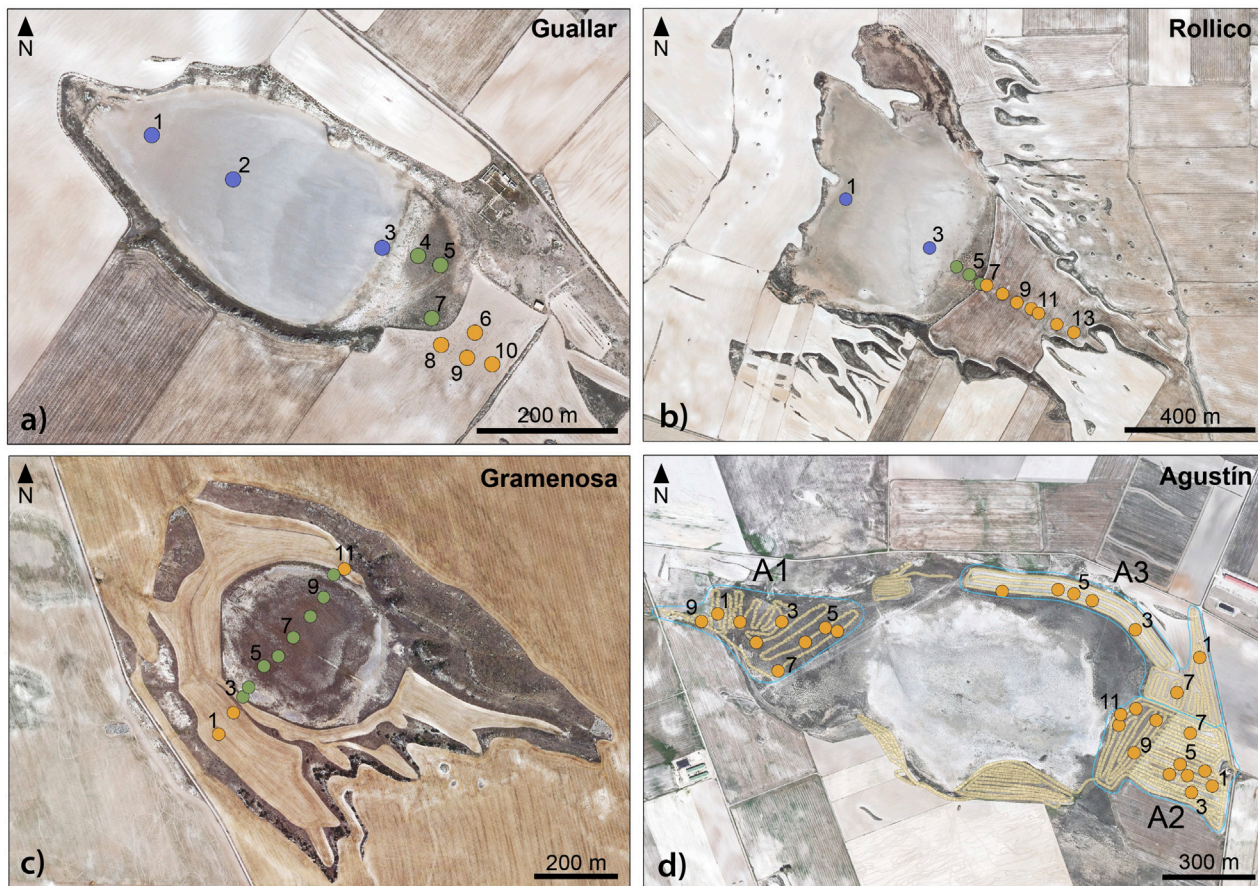


**FIGURE 2** | Distribution of soil sampling sites in the transects along the interface wetland-crop in Guallar (a), Rollico (b), Gramenosa (c) and in the agricultural plots (A1, A2, A3) around Agustín (d).

**TABLE 1** | Soil sampling characteristics along transects and within plots.

Parameter described	Wetland (salada) name			
	Guallar	Rollico	Gramenosa	Agustín
Length of the sampled transect (m)	612.4	803.9	453.5	---
Surface area of the sampled plots (ha)	---	---	---	A1: 10.3 A2: 15.9 A3: 8.2
Maximum difference in elevation (m)	Bottom: 0.03 Fringe: 2.37	Bottom: 0.13 Fringe: 8.09	Bottom: 0.26 Fringe: 4.67	A1: 2.42 A2: 1.81 A3: 2.55
Total number of sites sampled	10	13	11	A1: 9 A2: 12 A3: 7
Soil depth (cm) reached (*) min-max	Min 60 Max 260	Min 50 Max 125	Min 75 Max 150	A1: Min 90 max 150 A2: Min 40 max 120 A3: All to 120
Soil sampling intervals (cm)	20	20 or 25	25	25
Total number of soil samples	66	50	67	136
Land cover/land use	Bare/Nat.veg./Dryfarmed	Bare/Nat.veg./Dryfarmed	Nat.veg./Dryfarmed	Dryfarmed
Groundwater depth (cm)	31–226	Flooded-71	131–148	Not accessed

(\*) The soil depth (cm), minimum and maximum, reached with the hand auger in the points of the transect is illustrated in **Figure 6**.

We measured the groundwater depth and used a bailer-type sampler for taking water samples. Electrical conductivity (EC) and pH were determined in the field with the ORION 150A + conductivity meter and CRISON PH25 pH meter, respectively.

## Electromagnetic Sensor Readings and Calibration

Electromagnetic sensor (EMS) readings were taken with a hand-held Geonics EM38 sensor in points along wetland-crop transects in Rollico, Guallar, and Gramenosa. The readings were taken 9 days after a rain of 32.2 mm in the nearby Valfarta weather station (SIAR network<sup>2</sup>), in trafficable soil conditions. The rainfall was enough for the correct operation of EMS. The readings were taken on the same day in horizontal and vertical positions of the sensor, i.e., coils parallel and perpendicular to ground, respectively. The readings were corrected with the conversion table of US Salinity Laboratory Staff (1954) in order to reference them to 25 °C. Then these dimensionless numbers (Herrero et al., 2024), divided by 100, were termed EMH and EMV, respectively. In Agustín we used the electromagnetic sensor DualEm 1S operating in horizontal (EMh) and vertical (EMv) positions. After Urdanoy and Aragüés (2012), this sensor gives measurements basically similar to EM-38. The DualEm sensor was mounted on a plastic sled towed by a tractor at a distance of 3 m allowing the automatic acquisition of georeferenced readings. The sensor was connected to a Garmin Etrex GPS and an Allegro CX computer (Juniper Systems, USA), where the sensor readings were recorded and georeferenced in real time. A preliminary map of mobile EMS readings was created in the field using the ArcGIS® kriging tool in order to decide the soil sampling points.

EMh y EMv were used for estimating soil salinity as ECe and EC1:5 at different sampled depth intervals using linear regression (López-Bruna and Herrero, 1996; Nogués et al., 2006) up to 100 cm. For the plots, the best regression equation of ECe was applied on the raster image produced with the DualEm 1S horizontal readings to generate the corresponding soil salinity map.

## Laboratory Measurements and Data Analysis

Soil samples were dried at 30 °C–40 °C to avoid the loss of water from the gypsum ( $\text{CaSO}_4 \cdot 2\text{H}_2\text{O}$ ) and grounded and sifted through a sieve of 2 mm mesh diameter. In all the soils we determined the electrical conductivity (EC) of 1:5 and 1:10 soil:water extracts with the conductivity meter Orion 013605MD. The pH was measured using a pH electrode (Orion 9157BNMD), and the major ions were determined by chromatography (Metrohm 861 Advanced compact IC, Metrohm AG, Herisau, Switzerland). The EC of the saturation extract (ECe) was determined in all the samples of the transects and in a half of the samples (69) of

Agustín and it was estimated for the rest of Agustín samples using the regression of ECe on EC1:5.

The salinity profiles were analysed based on the EC1:5 extracts per sampling site using the original sampling depths. In order to compare the different sites, for each site we established a comparable depth up to 50 cm, as relevant for the cereal and vegetation roots activity, and to 100 cm to analyse possible influence of deeper layers or groundwater. The integrated salinity for these two depths was calculated by weighting the EC values by the thickness of each layer (Castañeda et al., 2012).

## RESULTS

### Landforms of the Saladas Previous to the Agricultural Intensification

The detailed geomorphological maps of the saline wetlands show a diversity of landforms, including lacustrine deposits associated with the flooded or vegetated bottoms and aeolian deposits on the leeward side of some of the saladas (Figure 3). The four studied saladas are inset into broader depressions usually framed by conspicuous flat-bottomed valleys excavated on the flat Miocene structural surface. The valleys network evidences structural and hydrological connection between neighboring depressions which stand out for their elongated shape in a NW-SE direction. Guallar (Figure 3a) develops along a NW-SE elongated depression with a major axis of about 1 km long and delimited to the northeast by a gypsum escarpment of about 10.4 m height that includes decimetric limestone strata. The flat bare lakebed extends to the aeolian deposit mainly covered by halophytes.

Rollico (Figure 3b) is inset within a relatively deep depression developed in the confluence of a wide structural surface developed to the NW and a pediment slope draining from the SW. The bare lakebed is enclosed by two lacustrine terraces, both of them less than 6 m high above the lake bottom, and by two adjacent aeolian deposits in the leeward zone. Gramenosa (Figure 3c) is part of a wider depression which includes a continuous colluvial deposit surrounding the main wetland and a small adjacent lakebed at the NW zone surrounded by vegetation. Agustín (Figure 3d) is located at the lowest topographic position of a complex area excavated into the largest flat-bottomed valley in the region, about 22 km long and 1.7 km of maximum width. The border of the depression hosting the wetland is blurred within the valley which includes a noticeable colluvium with a landslide to the north, together with small pediments. Leeward aeolian deposits are also present in the bottom of the depression.

The scarce elevation differences accounted along the transects (Table 1) provide evidence of the flatness of the saladas bottoms, especially in the bare soil of the playa lakes. A relatively higher topographic gradient is present along the vegetated fringe, varying from +2.4 m in Guallar to +8.1 m in Rollico. The fringe of Agustín around the vegetated bottom is relatively flat, with less than 2.5 m of elevation difference between the sampled sites.

<sup>2</sup><https://servicio.mapa.gob.es/websiar/SeleccionParametrosMap.aspx?dst=1>

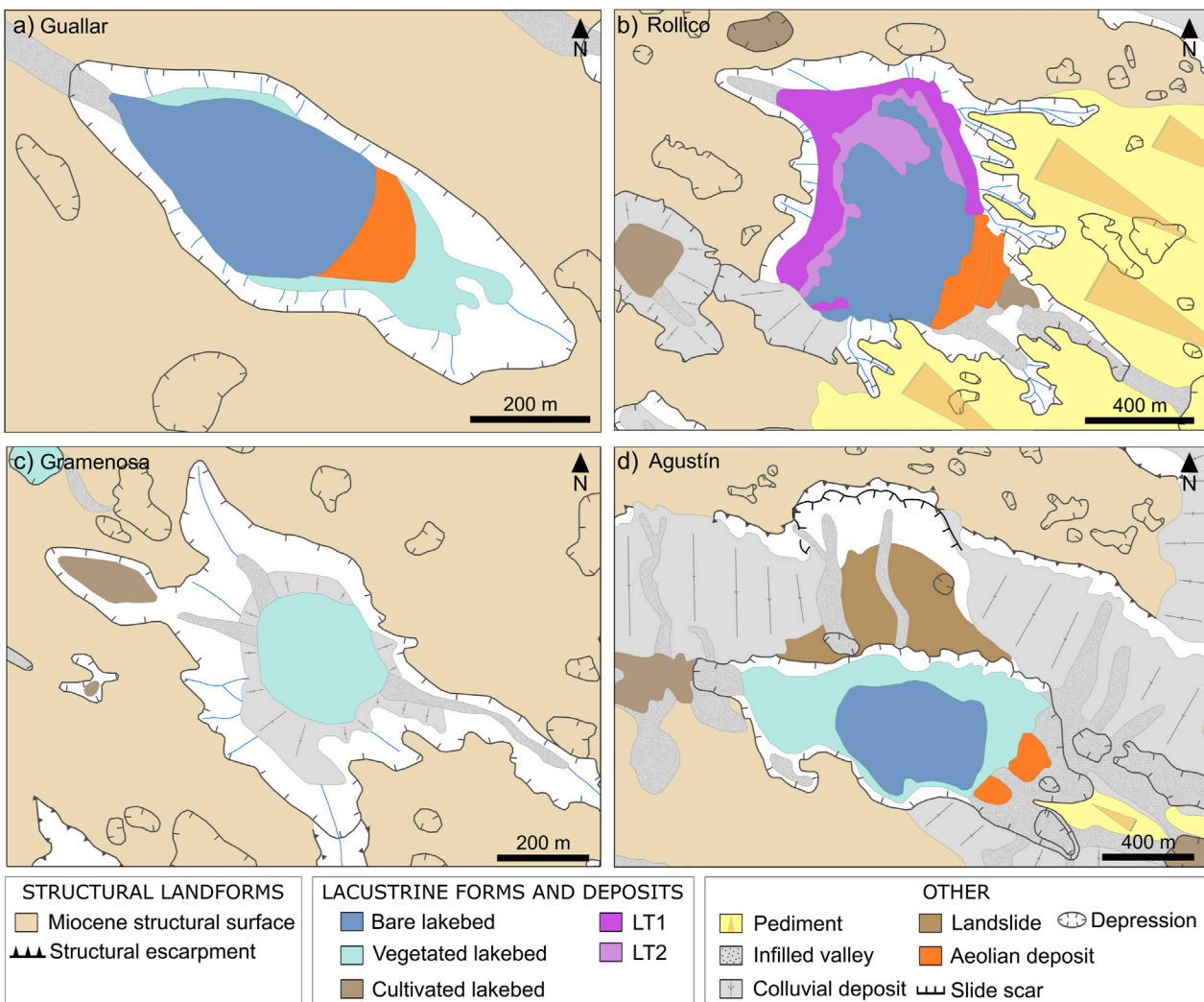


**FIGURE 3** | Geomorphological maps of the studied saladas: Guallar (a), Rollico (b), Gramenosa (c) and Agustín (d). Areas left in blank represent bare slopes where different substratum rocks outcrop (mainly gypsum and limestone).

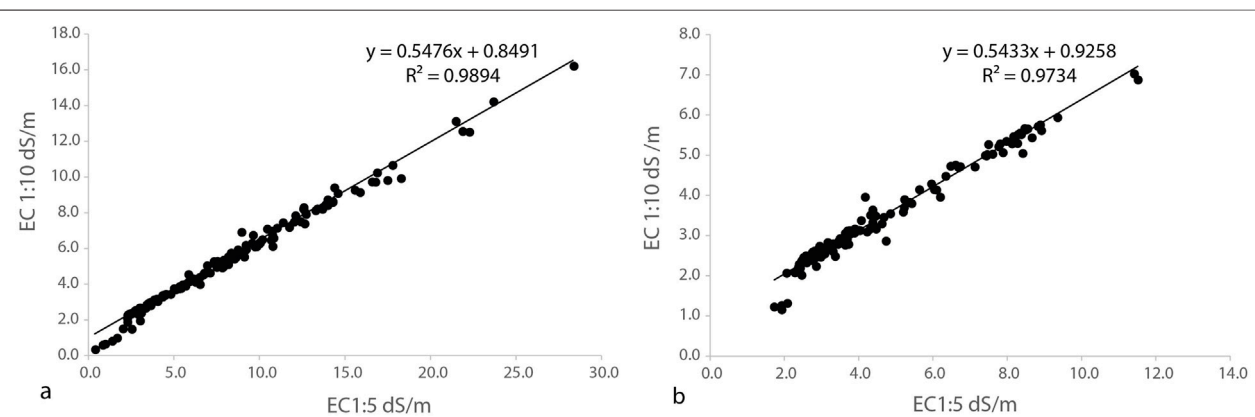
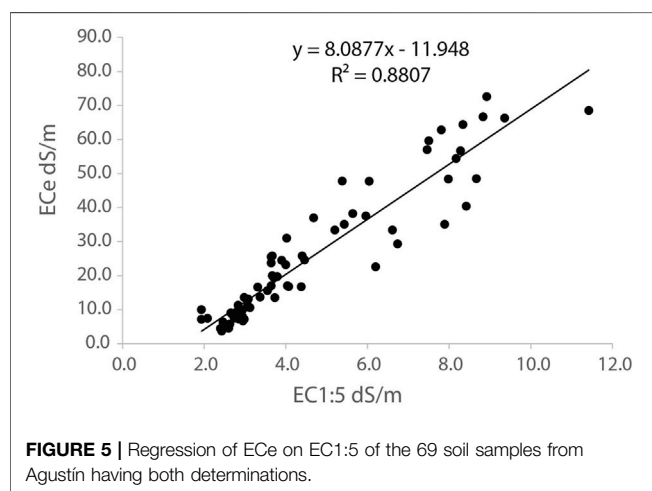


**FIGURE 4** | Regression of EC1:10 on EC1:5 in the soil transects (a) and the plots (b).



### Assessment of the Electrical Conductivity

The regression of the EC1:5 versus EC 1:10 values obtained an  $R^2 = 0.98$  in the transects and  $R^2 = 0.97$  in Agustín plots. In both cases, the group of points more deviating are from line and near the origin of coordinates, corresponding to the low salinity values, less than  $2.5 \text{ dS m}^{-1}$ . A line can be fitted well (Figure 4) even without eliminating the points with lower EC, which probably show the presence of gypsum or maybe of more soluble salts in an insufficient proportion to reach the concentration of the 1:5 extract in the 1:10 extract.

In Agustín plots, the regression of ECe on EC1:5 for the 69 samples with both determinations gives a determination coefficient of 88% (Figure 5), and a standard error of  $6.8 \text{ dS m}^{-1}$  and allows to estimate the ECe for all the Agustín samples with **Equation 1**:

$$ECe = 8.0877 \times EC1: 5 - 11.948 \quad (1)$$

### Spatial Distribution of Sol Salinity

Table 2 summarizes the soil salinity values for each salada as a whole and for each soil cover. The salinity shows a similar pattern in the three transects, in close relationship to the geomorphic position and the soil cover. The highest values occur in the bare soil bottom of the saladas (mean EC1:5 of about  $15 \text{ dS m}^{-1}$ ), the intermediate values are found in the fringe of vegetation (from  $6.5$  to  $10.2 \text{ dS m}^{-1}$ ), and the lowest values correspond to the soils of the crops (from  $3$  to  $4.6 \text{ dS m}^{-1}$ ). Apart from the averaged values, there are also differences in the range of the EC values along the transect in each salada. The transects along Guallar and Rollico playas-lakes collect the highest salinity range (up to  $27.7 \text{ dS m}^{-1}$ ) and a similar mean salinity at their bare bottom. The lowest mean salinity occurs in the vegetated saladas, Gramenosa and Agustín, with EC1:5 of  $5.7$  and  $4.6 \text{ dS m}^{-1}$ , respectively. Here the salinity range is about a third part of the range in the playas-lakes, about  $9 \text{ dS m}^{-1}$ .

The natural vegetation of Rollico fringe (Table 2) withstands higher salinity than that of Guallar or Gramenosa, not only by the mean but also the minimum EC values registered. The crops sampled along the transects exhibit also notable soil salinity, especially high in Agustín (mean  $4.6 \text{ dS m}^{-1}$ ), followed by Guallar and Gramenosa, with  $3.6 \text{ dS m}^{-1}$  and  $3.1 \text{ dS m}^{-1}$ , respectively.

Based on the ECe salinity phases of Nogués et al. (2006), a 73% of the soil samples are very strongly saline ( $ECe > 16 \text{ dS m}^{-1}$ ). They are spread in the saladas regardless of the soil cover, from the hypersaline bare soil of the playas-lakes to the crops. Similarly, most soil samples of the natural vegetation are very strongly saline. All the soil salinity phases, except the non saline, can be found in the cereal area: slightly (5%), moderately (14%), strongly (23%) and very strongly (58%) saline. Summarizing, half of the very strongly saline soils samples have been taken in agricultural areas with no soils free of salinity.

**TABLE 2** | Main statistics of soil salinity determined in all the soil samples in the different soil covers of the wetlands.

Wetland (salada)	EC1:5 (n = 319)			ECe (n = 319)		
	Mean (±st dev)	Max	Min	Mean (±st dev)	Max	Min
All soil covers						
Guallar	9.6 (±5.5)	28.40	1.69	72.1 (±41.2)	139.0	6.2
Rollico	7.5 (±5.2)	21.90	2.29	53.4 (±45.7)	126.9	2.8
Gramenosa	5.7 (±2.4)	9.64	0.41	37.0 (±21.0)	71.5	2.3
Agustín	4.6 (±2.2)	11.52	1.73	26.9 (±17.6)	77.0	3.7
Bare bottom						
Guallar	15.0 (±4.7)	28.40	9.58	116.7 (±12.9)	139.0	93.8
Rollico	15.4 (±3.0)	21.90	12.12	111.8 (±10.3)	126.9	93.5
Natural vegetation						
Guallar	7.6 (±1.5)	10.84	4.36	61.4 (±12.4)	78.9	33.2
Rollico	10.2 (±1.6)	12.72	7.35	88.9 (±13.4)	105.2	66.1
Gramenosa	6.5 (±1.8)	9.64	3.03	43.3 (±18.2)	71.5	8.6
Dryfarmed						
Guallar	3.6 (±0.8)	4.54	1.69	14.0 (±5.2)	21.5	6.2
Rollico	3.0 (±1.6)	4.03	2.29	10.7 (±7.7)	27.2	2.8
Gramenosa	3.1 (±2.0)	6.11	0.41	15.8 (±15.4)	38.7	2.3
Agustín	4.6 (±2.2)	11.52	1.73	26.9 (±17.6)	77.0	3.7

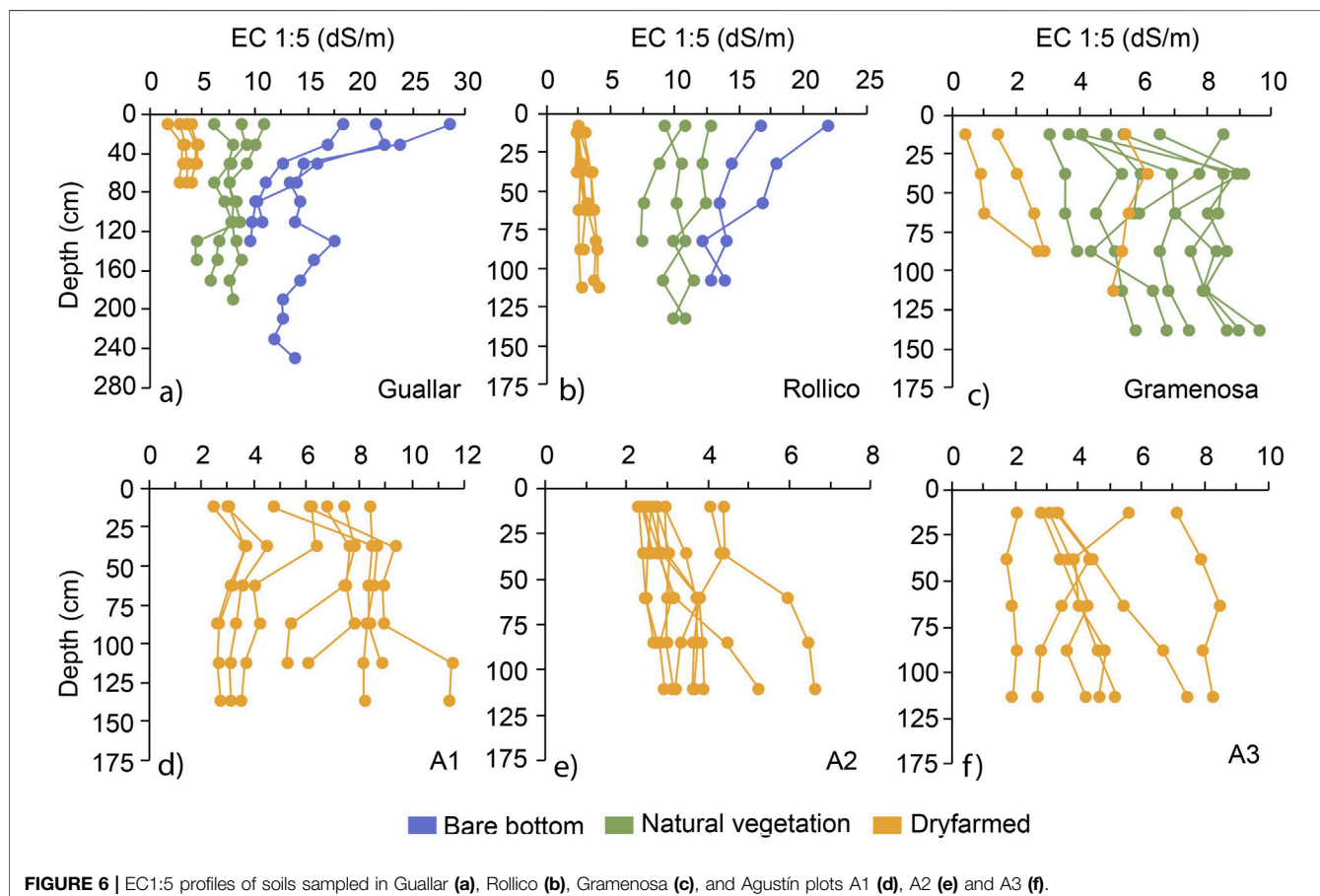


**FIGURE 6** | EC1:5 profiles of soils sampled in Guallar (a), Rollico (b), Gramenosa (c), and Agustín plots A1 (d), A2 (e) and A3 (f).

## Vertical Distribution of Soil Salinity

Figure 6 illustrates the vertical distribution of soil salinity (EC1:5) within each salada, along the transects and in the dryfarmed area fringing Agustín. Salinity profiles were analyzed to depths ranging from 60 to 260 cm. The soil depth reached was very variable and, in general, lower at sites located on the crop area of the transects. At Guallar (Figure 6a) the sampled depth uniformly decreased towards the crops whereas at Rollico (Figure 6b) a similar depth was sampled in all the sites along the transect. There is a noticeable variability of the vertical distribution of soil salinity along the transects though in general, the salinity profiles can be grouped by soil cover, especially the upper soil horizons. Deeper horizons show a heterogeneous salinity pattern since the changes may occur at different depths. In general, the range of the soil salinity values along each transect is maximum at the surface horizons and clearly decreases with soil depth, especially in Guallar and Rollico.

The salinity profiles of Agustín reached up to 150 cm having a relatively uniform sampled depth (Figures 6d-f). The vertical distribution of salinity is heterogeneous even in the same plot and presents no relationship to the elevation. Unlike the transects, the range of salinity values are similar at the surface and subsurface horizons. The highest depth (150 cm) and the highest salinity range, EC1:5 from 2.5 to 11.5 dS m<sup>-1</sup>, was reached at A1 plot

(Figure 6d). The salinity can be maximum at the surface horizon, constant along the profile or can increase with depth. Frequently, a higher salinity ranging from 3.4 to 9.4 dS m<sup>-1</sup> is observed in the first 50 cm. Only one point showed a considerable salinity increase deeper than 100 cm.

The saline profiles of A2 were quite uniform and represent a lower salinity range, from 2.3 to 6.6 dS m<sup>-1</sup>, with only two sites with EC increasing with depth. All the A3 plot profiles were slightly shorter (up to 120 cm) and, similar to A1, showed a diversity of vertical salt distribution and the surface horizon (25 cm) can be very strongly saline, with EC1:5 up to 7.3 dS m<sup>-1</sup>.

## Salinity and Depth of the Groundwater

Groundwater was reached in some of the sampled sites along the transects (Figure 7), at depths ranging from 31 to 195 cm (before equilibrium) plus one site flooded in Rollico bottom. Once stabilize, the water level was at ~140 cm in sites #5 to #9 in the vegetated bottom of Gramenosa, with a mean EC of 82.6 dS m<sup>-1</sup>; up to 25 cm at the bare bottom of Guallar (sites #1 to #3) and deeper (~190 cm) in the vegetated fringe (site #4), with 133 dS m<sup>-1</sup> mean EC; and at ~70 cm in the bare bottom and vegetated fringe of Rollico (sites #1 to #6), with a mean EC of 144.3 dS m<sup>-1</sup>. In general pH ranged from 6.8 to 7.3 and the anions composition was characterized by the high amount of chloride (54 g L<sup>-1</sup>) followed by sulfate (27 g L<sup>-1</sup>) with a ratio Cl/SO<sub>4</sub> of 2.7. The main

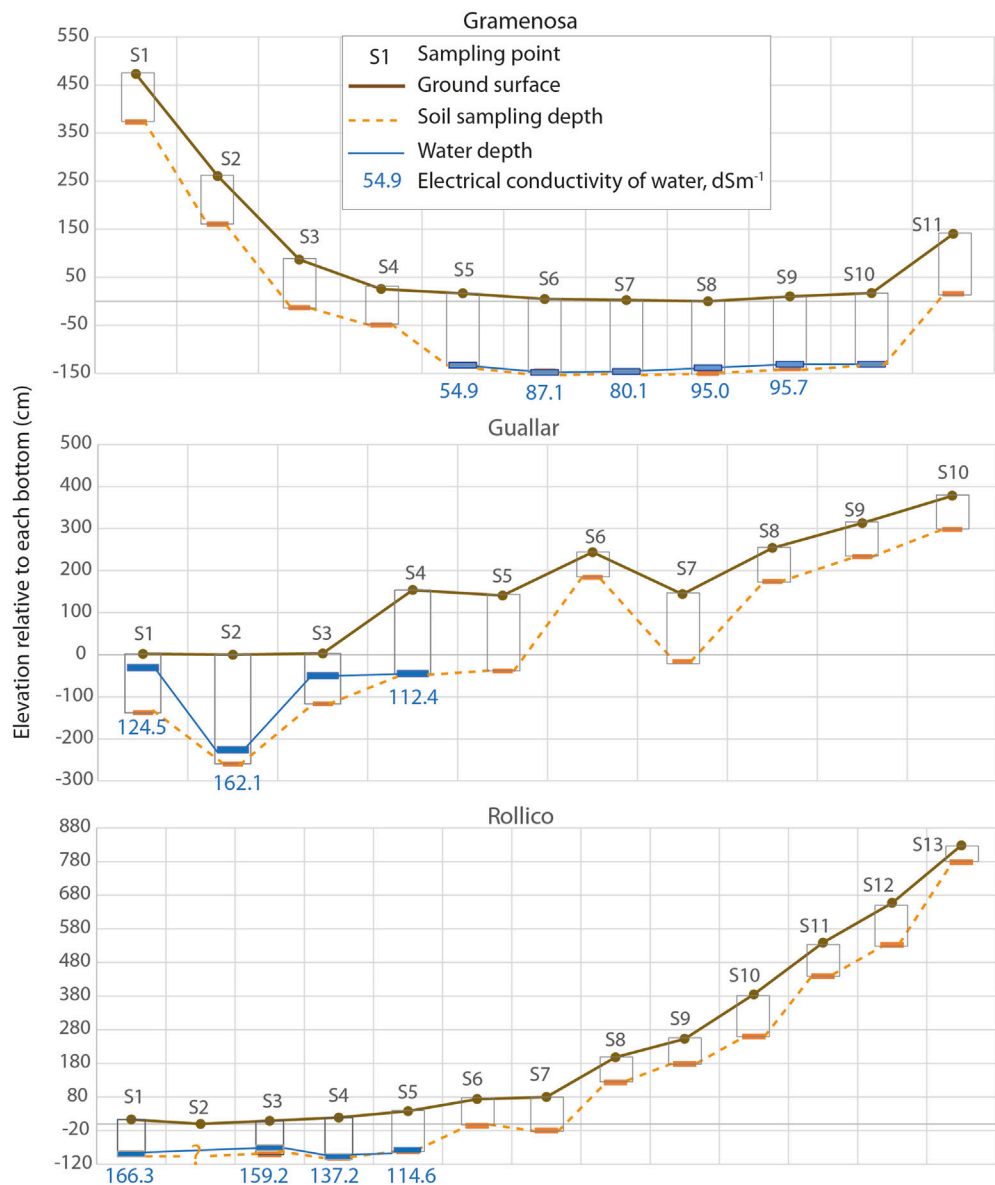


**FIGURE 7** | The topographic profiles of Gramenosa, Guallar and Rollico saladas with the sampling points and soil depth reached. Where available, the water depth and its electrical conductivity are indicated. Horizontal axis not to scale, Figure 2 for reference.

cations were sodium ( $21 \text{ g L}^{-1}$ ) followed by magnesium ( $8 \text{ g L}^{-1}$ ) with a mean ratio Mg/Ca of 20.1.

## Salinity Distribution in Integrated Soil Depths

**Figure 8** summarizes the soil salinity of the saturation extract (ECe) weighted up to 50 cm (ECe50) and 100 cm (ECe100). The overall distribution of EC values at the sampled sites was consistent with the expected salinity. A limited number of sites can be classified as slightly or moderately saline. The salinity range along the transects showed some differences between both soil depths. In general, ECe100 was higher than

ECe50, and the EC range of the vegetated saladas was not as wide as that of the playa-lakes. The ECe50 of the playa-lakes bottom can be twelve times that of the crops in Guallar and more than twenty times in Rollico. In these playa-lakes the ECe50 gradient was greater than that of ECe100 due to the high ECe50 values at their hypersaline bottom. The EC variability within Agustín plots can not be associated with systematic relevant topographic differences or the phreatic level.

The graphs of **Figure 8** show some local spots of unexpected high salinity, identified by the ECe of both depths. Most of these deviated points are located outside the salada bottom, in the leeward low-lying area of the aeolian deposits (orange in **Figure 3**) identified in Guallar

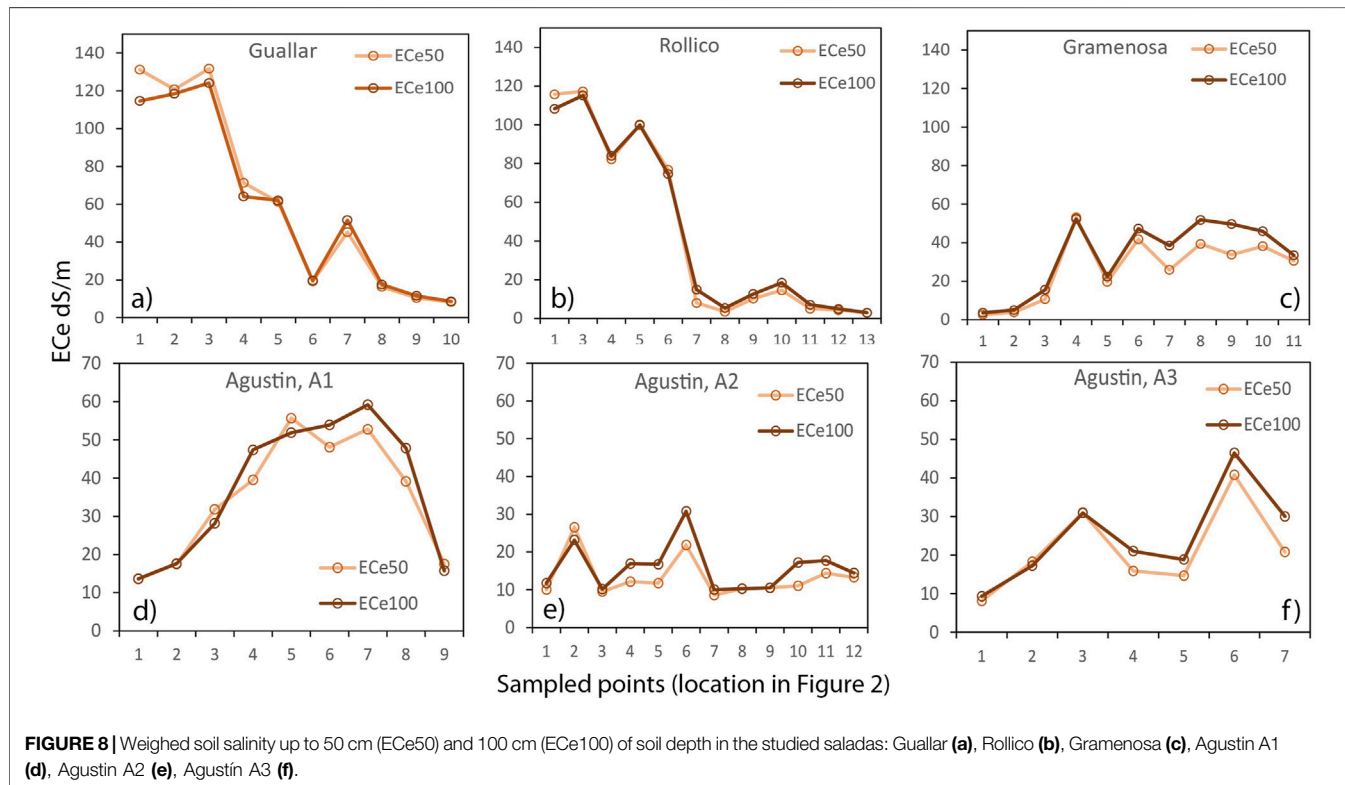


**FIGURE 8** | Weighed soil salinity up to 50 cm (ECe50) and 100 cm (ECe100) of soil depth in the studied saladas: Guallar (a), Rollico (b), Gramenosa (c), Agustín A1 (d), Agustín A2 (e), Agustín A3 (f).

(Figure 8a, site #7), Rollico (Figure 8b, sites #9, #10), and Agustín A2 (Figure 8e, sites #4 to #6). A similar saline spot occurs on the edge at Gramenosa (site #4) (Figure 2). The water table was never reached at these sites during sampling or during the visits in the following 3 months.

## Correlation Between EMS Readings and EC of Soil Extracts

The calibration of EMS to determine edaphic salinity in the studied transects, using the EC obtained from 1:5 and 1:10 soil extracts for integrated soil depths resulted in the equations summarized in Paracuellos (2006). The correlation analysis showed differences between the saladas (Figure 9). Only Rollico (Figures 9b,e) did not show differences in the coefficients of determination ( $R^2$ ) between horizontal and vertical readings. At Gramenosa (Figures 9c,f),  $R^2$  values were very low, the maximum being 4% in extract 1:5 at a depth of 0–20 cm. In both extracts, the regressions with EMh had higher determination coefficients than those with EMv for all depths. In 1:5 extract the best fit occurred up to the depth of 20 cm and became worse as depth increased, whereas in 1:10 extract the best fit occurred for the depth of 60 cm and thereafter  $R^2$  decreased with soil depth. At Guallar (Figures 9a,d),  $R^2$  values were acceptable for soil depths down to 80 cm (74%–87%), although there was a sharp decrease from this depth (45%–63%). The  $R^2$  values were higher for

settings with EMv (~81%) than with EMh (~69%). In Guallar the prediction EC1:5 values were established with the equation **Equation 2**,

$$EC1: 5 = 2.93 + 1.07 \times EMv \quad (2)$$

At Rollico (Figures 9b,e), for both extracts  $R^2$  increased with depth even though the number of points that influence is smaller and the standard error is also smaller (Paracuellos, 2006). The maximum  $R^2$  occurred at 100 cm, 94% and 96% at 1:5 and 1:10, respectively.  $R^2$  was higher at all depths in the 1:10 extract. No significant differences in  $R^2$  were observed in EMh and EMv.

For Guallar and Rollico the calibration equations corresponding to the 60 cm depth were appropriate because the salinity of this thickness was the most influential on cereal yield. They showed acceptable  $R^2$ , especially the 1:5 extracts (Figures 9a,b), whose values were 80% or higher. In Rollico, the calibration equation is **Equation 3**,

$$EC1: 5 = 2.53 + 0.63 \times EMh \quad (3)$$

The map of EMS readings (Figure 10) displayed a noticeable spatial variability within the Agustín plots. Higher  $R^2$  values were obtained for the EMh than for EMv. The  $R^2$  values were very low at the first layer (0–25), increasing from 0 to 50 cm. The correlation with EC1:5 was slightly better than with EC1:10. We selected the equation **Equation 4**,

$$ECe = 3.095 + 6.561 \times EMh \quad (4)$$

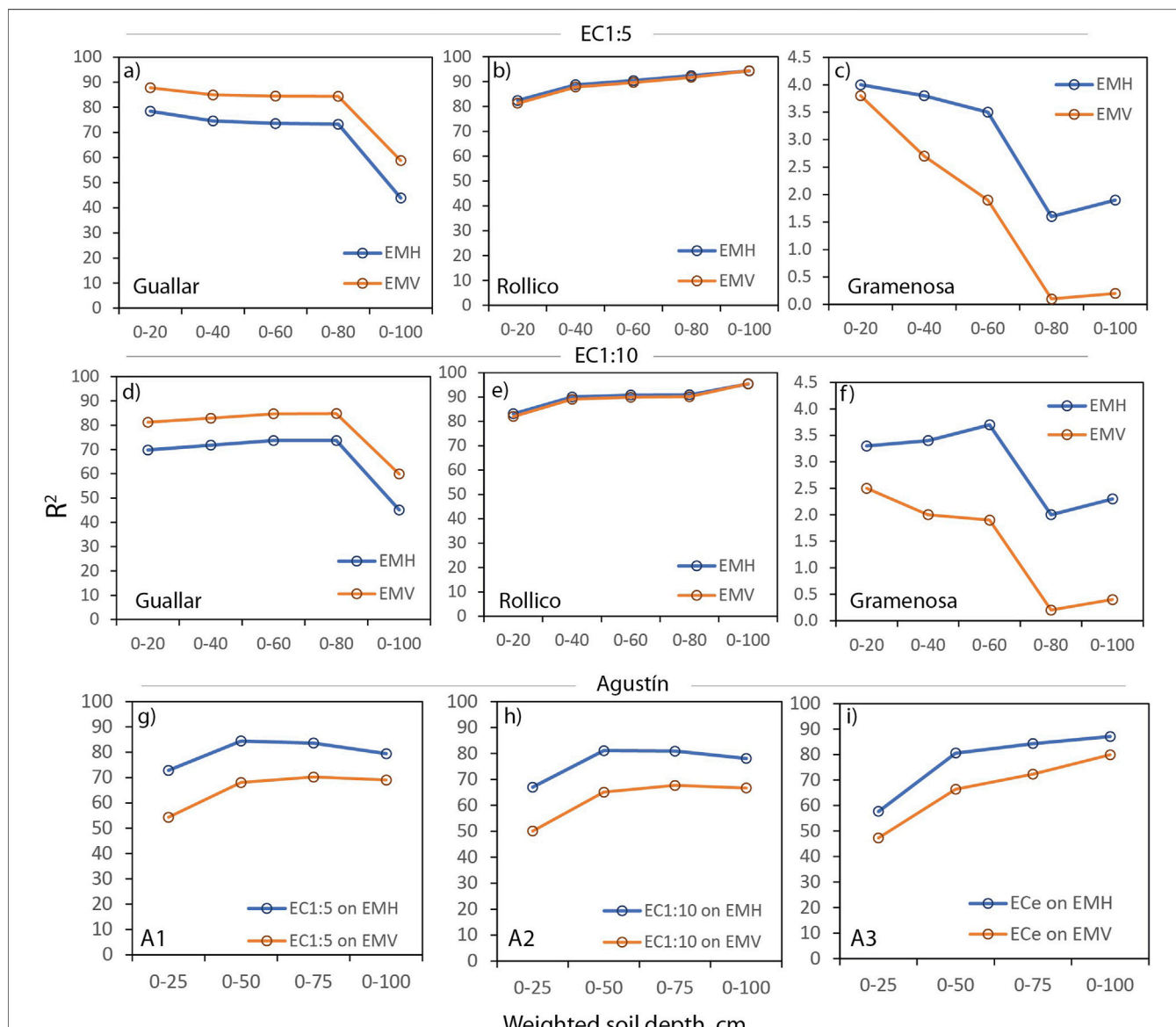


**FIGURE 9** | Coefficients of determination ( $R^2$ ) calculated for increasing soil depths.  $R^2$  obtained from the lineal regressions of EMS readings on EC 1:5 and EC 1:10 in Guallar (a,d), Rollico (b,e) and Gramenosa (c,f), respectively. And  $R^2$  obtained from ECe in Agustín A1 (g), A2 (h) and A3 (i).

with  $R^2 = 81\%$ , corresponding to the weighted ECe up to 50 cm depth, the zone where most roots responsible for nutrient absorption under irrigation usually grow (Isla, 2001).

The resulting salinity map provided soil salinity estimation at unsampled sites (Figure 11a) and allowed for a comprehensive description of the salinity distribution and comparisons between the surveyed areas. Almost the complete fringe of Agustín depicted ECe  $>4$  dS m $^{-1}$ . The salinity decreased towards the crops in areas with higher elevation, especially in A2, because at higher topographic positions the depth of the water table increased. This area exhibited the greatest spatial variability of salinity from the studied plots. A concentric distribution was

observed, with ECe  $>10$  dS m $^{-1}$  at the center and the rest of the area with values between 2 and 10 dS m $^{-1}$ . The higher values occurred at the leeward depression of the aeolian deposit (Figure 3d) currently cultivated though with limited production (Figure 11b).

## DISCUSSION

Soil salinity is well known as a threat in agricultural land (FAO, 2021) though the productive approach faces the occurrence of naturally saline soils even when they are unique and protected enclaves under international regulations (FAO, 2024). The

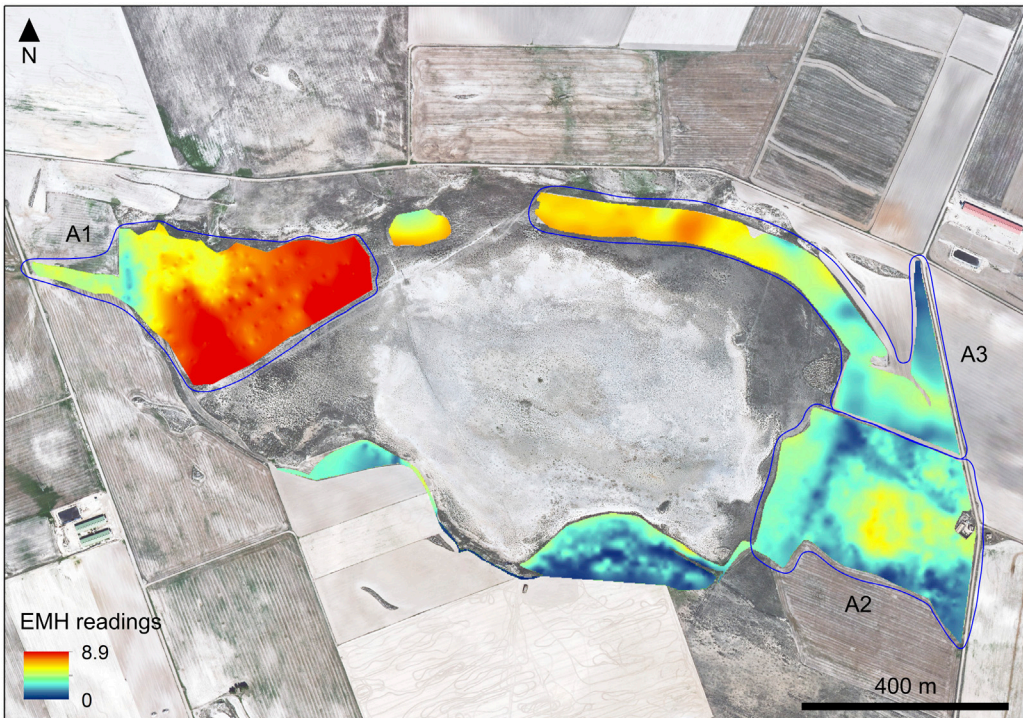


**FIGURE 10 |** Spatial variability of EMh values in the sampled plots around Agustín.

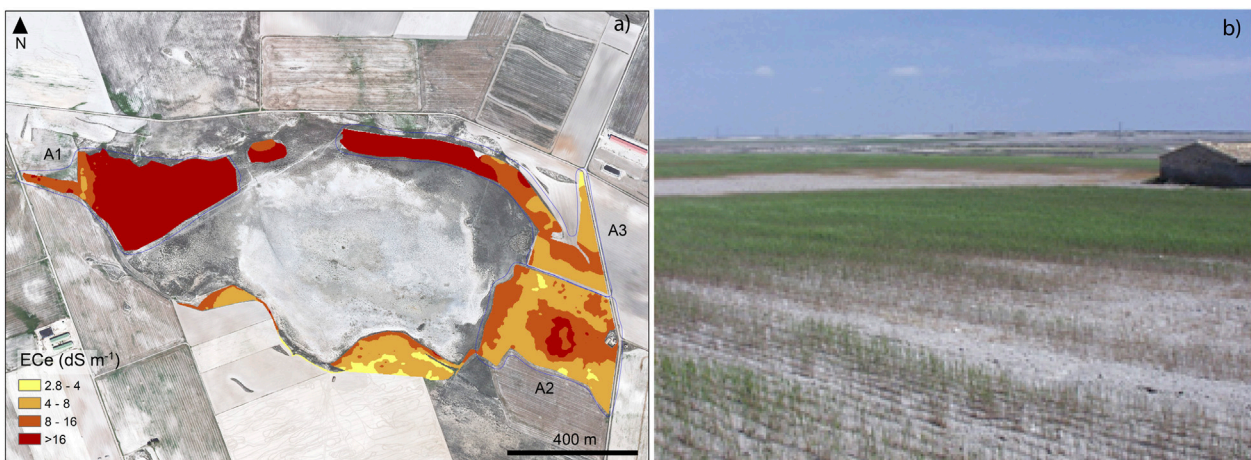


**FIGURE 11 | (a)** Salinity map (ECe) of the agricultural plots along the perimeter of the salada Agustín; **(b)** Field view the A2 plot in May 2008 showing in the foreground and background the limited growth of the wheat due to salinity.

saladas of Monegros are only an example of the co-occurrence of inland saline environments sharing conservation and production criteria.

## The Agricultural Landscape

A diversity of landforms was identified in the saladas area, covering about 230 km<sup>2</sup>, including halophytic vegetation in the saladas bottoms, aeolian deposits

associated with bare playas, sharp escarpments, nested or coalescent depressions and networks of flat-bottomed valleys, among others. The detailed geomorphological map, based on the aerial photographs from 1957, captured the geoforms under landscape conditions previous to the homogenization produced by the transformations carried out to install the new irrigation (Domínguez-Beisiegel et al., 2013a).

A smoothed and homogeneous landscape was found during the soil surveys especially due to the land consolidation and excavation works for irrigation and drainage pipes. Following the disappearance of many of the saladas, the area now shows larger and more continuous agricultural fields free of vegetated fringes and with a great number of new intensive pig farms (Tierra et al., 2025). Under this scenario, the original mapped landforms (**Figure 3**) are key for interpreting the distribution of soil salinity and the frequent occurrence of superficial color patches with distinct soil properties (Castañeda and Moret-Fernández, 2013).

Similar transformations occurred in other semiarid environments in the CEB, such as the saladas of Alcañiz-Calanda, among others, and in other regions of Spain and saline environments worldwide usually requiring *in situ* knowledge to predict salinization effects and prevent degradation (Tedeschi, 2020).

## Electrical Conductivity and Sampling Approaches

The EC of the saturation extracts is a worldwide accepted method established by the US Salinity Laboratory Staff (1954), originally aimed at agriculture for expressing soil salinity. We applied it in wetland ecosystems for meaningful comparisons in the continuum of habitats at the interface with agriculture. The EC determined in the two extracts, 1:5 and 1:10, are robust as showed by the relationships between them. The relationship between the ECe and EC1:5 is similar to that obtained by Herrero et al. (2015) computing 359 samples from 10 saladas not coincident with the ones studied in the present article. The regression result of ECe on EC1:5 in Agustín plots ( $R^2 = 88\%$ ) is comparable to that obtained for soils from the vegetated bottom of Agustín by Herrero (2008).

The response of EMS in Agustín presents the best relationship with a soil depth of 0–100 cm in A3 and with EMh readings (**Figure 9f**) although the relative contribution of the deep soil layers to the SEM readings is greater for the vertical position of the receiving coil (Abdu et al., 2007). These authors established a sensitive depth of exploration twice for vertical than for horizontal modes in a similar sensor. Yao and Yang (2010) proposed independent equations for each depth but Huang et al. (2015) considered that it is not necessary.

In Gramenosa, no acceptable fit was obtained, with low  $R^2$  values. Despite this, the graphs obtained maintain a relationship in their form, and the regression equations show a certain consistency, indicating that the results could be more favorable if the number of observations increased. In Guallar, the fit was generally good, with  $R^2$  values sharply dropping from 80 cm onward, possibly due to the smaller number of points or the influence of deeper layers. This is confirmed by the higher  $R^2$  values in EMv, where the relative contribution of deeper layers is greater. Rollico provided a good fit for all depths and with great uniformity, even though the number of computed points decreased with depth.

The transect method is an appropriate approach to explore the soil salinity in the flat landscape of Monegros with scattered depressions. The inclusion of the gradients of salt-tolerant vegetation in the transects made it possible to capture a representative range of salinity. The resulting salinity range

detected along the studied transects (from 9 to 26 dS m<sup>-1</sup>) (**Figure 6**) can be used as a model to be extrapolated to all the area hosting about 150 depressions and halophytes (Conesa et al., 2011; Castañeda et al., 2013) with the help of digital mapping techniques together with soil salinity proxies (Zhang et al., 2011).

The geomorphological features, including topography, govern the movement and distribution of soil salinity as they condition how and where water flows accumulates. In this sense, the spatial distribution of salinity together with appropriate geomorphological maps (**Figure 3**) are very useful to predict the effects of irrigation and salt mobilization at the landscape scale (Duncan et al., 2008). On the other hand, the salinity maps based on calibrated mobile EMS readings are advantageous for continuous information of soil salinity, though the vehicle approach is restricted to accessible areas, e.g., agricultural plots or other semi-urban environments (Williams et al., 2024), not frequently found in natural areas.

## Soil Salinity Variability at the Wetland-Crop Interface

The integrated salinity (**Figure 8**) allows comparing sites, soil covers, and saladas. The irregular soil salinity in relatively small agricultural plots (**Figures 8d–f**) with no relevant elevation differences could be related to the proximity of deeper saline layers even if no groundwater was reached on the sampling dates. García-Vera (1996) identified in Agustín the confluence of two aquifers in the area having dissimilar characteristics. Salvany et al. (1996) documented the frequent change of geological materials and groundwater characteristics at distances of few meters in the area, and the occurrence of local increases in salinity at the saladas fringe due to variable-density effects of groundwater. Besides, a great number of tectonic joints and the occurrence of preferential flows probably contributes to the heterogeneity of the subsurface materials yielding differences in soil salinity at distances of just a few meters.

Regarding the salinity profiles of **Figure 6**, one of the differences between the playa lakes and the agricultural plots is the striking high salinity range of the upper horizons in natural areas. The high ET<sub>0</sub> favors the capillary rise and evaporation through the bare soil (Castañeda and García-Vera, 2008) and subsequent salt accumulation in the upper layers, generating hypersaline areas that intensify the salinity gradient. On the contrary, the agricultural practices in the plots of Agustín very probably have a homogenizing effect on the upper layers of the soil profile (Ohigashi et al., 2025). To comply with CAP measures, continuous tillage is required under rainfed, even under long fallow practices (16–18 months).

Low values of Gramenosa may depend on the points chosen. Irregular salinity values in vegetated areas may be related to the higher density of the vegetation cover and the abundance of nitrophilous plants interspersed with the salinity-driven plant succession. Under these conditions, the soil cover changes cannot be precisely distinguished when selecting sampling sites. Sampling more closely aligned with lateral variation in soil salinity would require a prior study of plant distribution at a very detailed scale.

The salinity intervals for soil salinity classes (Nogués et al., 2006) were designed for agricultural soils and leave the samples with

ECe  $>16$  dS m $^{-1}$  in a single group, that is, 73% of the 319 samples studied. Regarding these intervals, new considerations would be needed to integrate the agricultural and ecological perspectives into the study of soil salinity in hypersaline areas.

## The Agronomic Perspective

The surface extent affected by salinity of **Figure 11a** can be quantified for individual CAP parcels of the interface between crops and the protected habitats. For agronomic application, a production criterion could be applied to establish a reference limit of production for each parcel (Serrate, 2009). As an example, Royo and Abió (2003) established as criterion a 50% decrease in durum wheat and barley yield due to the presence of salts in the soil. The authors obtained a mean salinity value (EC50) of 11.3 dS m $^{-1}$  as a limiting factor. EC50 is the electrical conductivity of saturation extract, which reduces yield to half of what would be obtained under non-saline soil conditions. This value would be more restrictive than that of barley, which can tolerate much higher salinity levels, with EC50 = 18 dS m $^{-1}$  (Ayers and Westcott, 1985). In this context, a proposal for a new agri-environment-climate measure could include qualifying plots with ECe  $>10$  dS m $^{-1}$  in more than 50% of the surface area. These plots could be considered not suitable for cultivation such as that of **Figure 10b**.

Some of the CAP greening obligations are to be monitored using the Land Parcels System (LPIS). Since part of the CAP subsidies to farmers are to be paid for agricultural practices beneficial for the climate and environment (e.g., benefit biodiversity, habitat restoration and maintenance, or retain landscape features), the plots of limited agricultural potential may form part of a new category of eligible areas within the LPIS as non-productive areas prone to natural variable salinity as proposed by Serrate (2009). Moreover, as recommended by European Court of Auditors (European Court of Auditors, 2016) to accurately identify this type of land as eligible, targeted on-the-spot data may be required, and this requirement is well suited for soil salinity due to their intrinsic temporal variability.

## CONCLUSION

This study carried out in the Saladas of Sástago-Bujaraloz presents an approach applicable to semiarid agricultural areas within Natura 2000 sites. All the surveyed soils, including bare, vegetated, fallow or cultivated, are saline, with EC ranging from slightly to very strongly saline. The results obtained about the spatial and vertical distribution of soil salinity show the complexity of the area, paralleling the hydrological complexity documented by previous studies. There is a highly variable salinity within a few metres of distance, especially in the plots of Agustín declared as eligible under LPIS. Guallar, Rollico and Gramenosa show a similar salinity pattern along the transects, and also include eligible very saline plots.

Both manual sampling along topographic transects and EMS readings across flat areas are suitable methodologies for use on this and similar environments with limiting conditions for production. The calibrated salinity maps provide a more complete view of soil salinity in order to quantitatively delimit

non-productive areas in the context of CAP regulations. A proposal for a new agri-environment-climate measure could include classifying plots with ECe  $>10$  dS m $^{-1}$  in more than 50% of the area as unsuitable for cultivation.

A diversity of landscape forms and associated processes were identified and mapped despite the general flatness of the area. The landscape features control the water flows and the accumulation of salts in the soil and subsoil, and the next fresh water inputs under new irrigation schemes will increase this potential. The characterization of landforms may allow for a qualitative estimation of new areas prone to salinization under irrigation. Future investigations should include appropriate water flow models for a better understanding of salinity distribution and irrigation effects. This knowledge may help in mitigating salt mobilization and preventing the salinization of productive areas.

## DATA AVAILABILITY STATEMENT

The raw data supporting the conclusions of this article will be made available by the authors, without undue reservation.

## AUTHOR CONTRIBUTIONS

MT, CC, and FJ participated in the design, interpretation of the studies and analysis of the data and ETM performed the data curation and organization. MT, CC, and FJG participated on the review of the manuscript; CC managed the project administration and funding acquisition. All authors contributed to the article and approved the submitted version.

## FUNDING

The author(s) declared that financial support was received for this work and/or its publication. This research was possible by the grant TED2021-130303B-I00 funded by MCIN/AEI/10.13039/501100011033 and by the “European Union NextGenerationEU/PRTR”, and the grant PID2021-127170OB-I00 funded by MCIN/AEI/10.13039/501100011033 and by “ERDF A way of making Europe”.

## CONFLICT OF INTEREST

The authors(s) declared that this work was conducted in the absence of any commercial or financial relationships that could be construed as a potential conflict of interest.

## GENERATIVE AI STATEMENT

The author(s) declared that generative AI was not used in the creation of this manuscript.

Any alternative text (alt text) provided alongside figures in this article has been generated by Frontiers with the support of

artificial intelligence and reasonable efforts have been made to ensure accuracy, including review by the authors wherever possible. If you identify any issues, please contact us.

## ACKNOWLEDGEMENTS

We would like to thank J. Herrero for his conceptual basis for developing this study and L. Serrate and E.

## REFERENCES

Abdu, H., Robinson, D. A., and Jones, S. B. (2007). Comparing Bulk Soil Electrical Conductivity Determination Using the DUALEM-1S and EM38-DD Electromagnetic Induction Instruments. *Soil Sci. Soc. Am. J.* 71 (1), 189–196. doi:10.2136/sssaj2005.0394

Ayers, R. S., and Westcott, D. W. (1985). “Water Quality for Agriculture,” in *FAO Irrigation and Drainage Paper No.29*. Rome: FAO. Available online at: <https://www.fao.org/4/t0234e/t0234e00.htm>.

Castañeda, C. (2002). El Agua De Las Saladas De Monegros Sur Estudiada Con Datos De Campo Y De Satélite. *Cons. Protección la Nat. Aragón* 35, 158. Available online at: <http://hdl.handle.net/10261/399164>

Castañeda, C., and García Vera, M. A. (2008). Water Balance in the Playa-Lakes of an Arid Environment, Monegros, NE Spain. *Hydrogeology J.* 16, 87–102. doi:10.1007/s10040-007-0230-9

Castañeda, C., Herrero, J., and Casterad, M. A. (2005). Landsat monitoring of playa-lakes in the Spanish Monegros Desert. *J. Arid Environ.* 63, 497–516. doi:10.1016/j.jaridenv.2005.03.021

Castañeda, C., and Moret-Fernández, D. (2013). Superficial Color Patches as a Visual Diagnostic Criterion for Agricultural Management. *Pedosphere* 23 (6), 740–751. doi:10.1016/s1002-0160(13)60066-1

Castañeda, C., Mendez, S., Herrero, J., and Betrán, J. (2009). “Investigating Soils for Agri-Environmental Protection in Arid Spain,” in *Land Degradation and Desertification: Assessment, Mitigation and Remediation*. Editor P. Zdruli (Springer–Verlag). doi:10.1007/978-90-481-8657-0\_41

Castañeda, C., Latorre, B., and Herrero, J. (2012). SLICES Versión 2.0; Synthetic Layers of Soil. doi:10.20350/digitalCSIC/9000

Castañeda, C., Herrero, J., and Conesa, J. A. (2013). Distribution, Morphology and Habitats of Saline Wetlands: A Case Study from Monegros. *Geol. Acta* 11 (4), 371–388. doi:10.1344/105.000002055

Casterad, M. A., Herrero, J., Betrán, J. A., and Ritchie, G. (2018). Sensor-Based Assessment of Soil Salinity During the First Years of Transition from Flood to Sprinkler Irrigation. *Sensors* 18 (2), 616. doi:10.3390/s18020616

Conesa, J. A., Castañeda, C., and Pedrol, J. (2011). “Las Saladas De Monegros Y Su Entorno: Hábitats Y Paisaje Vegetal,” in *Consejo De Protección De La Naturaleza De Aragón*. Zaragoza, 540. Available online at: <http://hdl.handle.net/10261/109666>.

Corwin, D. L., and Scudiero, E. (2019). Review of Soil Salinity Assessment for Agriculture Across Multiple Scales Using Proximal And/Or Remote Sensors. *Adv. Agron.* 158, 1–130. doi:10.1016/bs.agron.2019.07.001

Cuchi, J. A. (1986). *Aportaciones al conocimiento de los suelos salinos de Aragón*. Zaragoza: Estación Experimental de Aula Dei (EEAD-CSIC). Available online at: <http://hdl.handle.net/10261/184404>.

Dominguez-Beisiegel, M., Herrero, J., and Castañeda, C. (2013a). Saline Wetlands Fate in Inland Deserts: An Example of Eighty Years Decline From Monegros, Spain. *Land Degrad. & Dev.* 24 (3), 250–265. doi:10.1002/lrd.1122

Dominguez-Beisiegel, M., Castañeda, C., and Herrero, J. (2013b). Two Microenvironments at the Soil Surface of Saline Wetlands in Monegros, Spain. *Soil Sci. Soc. Am. J.* 77 (2), 653–663. doi:10.2136/sssaj12.0014

Duncan, R. A., Bethune, M. G., Thayalakumaran, T., Christen, E. W., and McMahon, T. A. (2008). Management of Salt Mobilisation in the Irrigated Landscape – A Review of Selected Irrigation Regions. *J. Hydrology* 351, 238–252. doi:10.1016/j.jhydrol.2007.12.002

Paracuellos for their commitment and academic research work in our group. We also acknowledge the assistance of the field technicians of the RAMA research group (<https://grupo-rama.es/en/home-english/>), especially to M. Izquierdo. We thank the Scientific and Technique Analysis Services in Pyrenean Institute of Ecology-CSIC in Zaragoza-Jaca (Spain) for their technical support. We acknowledge the comments of the two reviewers that helped to improve the manuscript.

European Court of Auditors (2016). *The Land Parcel Identification System: a useful tool to determine the eligibility of agricultural land - but its management could be further improved (Special Report 25/2016)*. Luxembourg: Publications Office of the European Union. Available online at: [https://www.eca.europa.eu/lists/ecadocuments/sr16\\_25/sr\\_lpis\\_en.pdf](https://www.eca.europa.eu/lists/ecadocuments/sr16_25/sr_lpis_en.pdf).

FAO (2021). *Global Map of Salt-Affected Soils Gsasmap v1.0*. Rome, Italy: FAO, 20. Available online at: <https://www.fao.org/documents/card/en/cb7247en>.

FAO (2024). Global Status of Salt-Affected Soils. *Main. Report*. doi:10.4060/cd3044en

García-Vera, M. A. (1996). Hidrogeología De Zonas Endorreicas En Climas Semiáridos: Aplicación a Los Monegros (Zaragoza Y Huesca). *Cons. Protección la Nat. Aragón* 3, 297.

Herrero, J. (2008). Salinidad Edáfica En Varios Salobrados De Aragón. *Memorias De La Real Sociedad Española De Historia Natural. Tomo IV*, 177. Available online at: <http://hdl.handle.net/10261/61398>.

Herrero, J., and Pérez-Coveta, O. (2005). Soil Salinity Changes over 24 Years in a Mediterranean Irrigated District. *Geoderma* 125 (3-4), 287–308. doi:10.1016/j.geoderma.2004.09.004

Herrero, J., and Snyder, R. L. (1997). Aridity and Irrigation in Aragon, Spain. *J. Arid Environ.* 35, 535–547. doi:10.1006/jare.1996.0222

Herrero, J., Artieda, O., and Hudnall, W. H. (2009). Gypsum, a Tricky Material. *Soil Sci. Soc. Am. J.* 73 (6), 1757–1763. doi:10.2136/sssaj2008.0224

Herrero, J., Weindorf, D. C., and Castañeda, C. (2015). Two Fixed Ratio Dilutions for Soil Salinity Monitoring in Hypersaline Wetlands. *PLoS ONE* 10 (5), e0126493. doi:10.1371/journal.pone.0126493

Herrero, J., López-Bruna, D., and Predebon, I. (2024). What Do Electromagnetic Sensors Measure in Soil Surveys? *Adv. Agron.* 187, 1–19. doi:10.1016/bs.agron.2024.05.001

Huang, J., Mokhtari, A. R., Cohen, D. R., Monteiro-Santos, F. A., and Triantafilis, J. (2015). Modelling Soil Salinity Across a Gilgai Landscape by Inversion of EM38 and EM31 Data. *Eur. J. Soil Sci.* 66 (5), 951–960. doi:10.1111/ejss.12278

Isla, R. (2001). *Efecto De La Salinidad Sobre La Cebada (Hordeum Vulgare L.). Análisis De Caracteres morfo-fisiológicos Y Su Relación Con La Tolerancia a La Salinidad*. Tesis doctoral. Lleida, Spain: Universidad de Lleida, 100. Available online at: <http://hdl.handle.net/10803/8324>.

López-Bruna, D., and Herrero, J. (1996). El Comportamiento Del Sensor Electromagnético Y Su Calibración Frente a La Salinidad Edáfica. *Agronomie* 16, 95–105. doi:10.1051/agro:19960203

McAneney, M. C., and Arrúe, J. L. (1993). A wheat-fallow Rotation in Northeastern Spain: Water balance-yield Considerations. *Agronomie* 13 (6), 481–490. doi:10.1051/agro:19930604

McNeill, J. D. (1991). Advances in Electromagnetic Methods for Groundwater Studies. *Geoexploration* 27 (1–2), 65–80. doi:10.1016/0016-7142(91)90015-5

Nogués, J., Robinson, D. A., and Herrero, J. (2006). Incorporating Electromagnetic Induction Methods into Regional Soil Salinity Survey of Irrigation Districts. *Soil Sci. Soc. Am. J.* 70, 2075–2085. doi:10.2136/sssaj2005.0405

Ohigashi, T., Madegwa, Y. M., Karuku, G. N., Njira, K., Uchida, Y. (2025). Agricultural land use induces broader homogenization of soil microbial functional composition than taxonomic composition in sub-Saharan Africa. *Soil Biol. Biochem.* 209, 109895. doi:10.1016/j.soilbio.2025.109895

Paracuellos, E. (2006). Medida Y Evaluación De La Salinidad Edáfica En Monegros Para Modulación De Las Ayudas De La PAC Por Superficies. Available online at: <http://hdl.handle.net/10261/372938>.

Pedrocchi, C., and Sanz, M. A. (1991). El Sistema Endorreico De Monegros: Un Ecosistema En Vías De Extinción. *Lucas Mallada* 3, 93–106. Available online at: <https://revistas.iea.es/index.php/LUMALL/article/download/940/937>.

Ramsar Convention Secretariat (2010). *Ramsar Handbooks for the Wise Use of Wetlands*. 1. Gland (Switzerland): Ramsar Convention Secretariat, 56.

Rhoades, J. D., and Corwin, D. L. (1981). Determining Soil Electrical- Conductivity Depth Relations Using an Inductive Electromagnetic Soil Conductivity Meter. *Soil Sci. Soc. Am. J.* 45 (2), 255–260. doi:10.2136/sssaj1981.03615995004500020006x

Royo, A., and Abió, D. (2003). Salt Tolerance in Durum Wheat Cultivars. *Span. J. Agric. Res.* 1 (3), 27–35. doi:10.5424/sjar/2003013-32

Salvany, J. M., García-Vera, M. A., and Samper, J. (1996). Geología E Hidrogeología De La Zona Endorreica De Bujaraloz-Sástago (Los Monegros, Provincias De Zaragoza Y Huesca). *Acta Geol. Hisp.* 30 (4), 31–50. Available online at: <https://revistes.ub.edu/index.php/ActaGeologica/article/view/4578>.

Serrate, L. (2009). *Estudio De Rasgos Edáficos Para Plantear Una Nueva Medida Agroambiental En Monegros Sur*. Spain: Universidad de Zaragoza. Available online at: <http://hdl.handle.net/10261/172060>.

Tedeschi, A. (2020). Irrigated Agriculture on Saline Soils: A Perspective. *Agronomy* 10, 1630. doi:10.3390/agronomy10111630

Tierra, M., Olarieta, J. R., and Castañeda, C. (2025). An Assessment of the N Load from Animal Farms in Saline Wetland Catchments in the Ebro Basin, NE Spain. *Land* 14 (6), 1170. doi:10.3390/land14061170

Tóth, G., Adhikari, K., Várányay, G., Tóth, T., Bódis, K., and Stolbovoy, V. (2008). “Updated Map of Salt Affected Soils in the European Union,” in *Threats to Soil Quality in Europe (EUR 23438, Issue May)*. Editors G. Tóth, L. Montanarella, and E. Rusco (Ispra, Italy: Office for Official Publications of the European Communities). doi:10.2788/8647

Urdanoz, V., and Aragüés, R. (2012). Comparison of Geonics EM38 and Dualem 1S Electromagnetic Induction Sensors for the Measurement of Salinity and Other Soil Properties. *Soil Use Manag.* 22 (1), 108–112. doi:10.1111/j.1475-2743.2011.00386.x

US Salinity Laboratory Staff (1954). Diagnosis and Improvement of Saline and Alkali Soils. *Agric. Handb.* 60. Available online at: [https://www.ars.usda.gov/ARSUserFiles/20361500/hb60\\_pdf/hb60complete.pdf](https://www.ars.usda.gov/ARSUserFiles/20361500/hb60_pdf/hb60complete.pdf).

Williams, D. M., Straw, C. M., Smith, A. P., Watkins, K. L., Hong, S. G., Floyd, W. F., et al. (2024). Using Electromagnetic Induction to Inform Precision Turfgrass Management Strategies in Sand-Capped Golf Course Fairways. *Agrosyst. Geosci. Environ.* 7, e70020. doi:10.1002/agg2.70020

Yao, R., and Yang, J. (2010). Quantitative Evaluation of Soil Salinity and Its Spatial Distribution Using Electromagnetic Induction Method. *Agric. Water Manag.* 97, 1961–1970. doi:10.1016/j.agwat.2010.02.001

Zhang, T. T., Zeng, S. H., Gao, Y., Ouyang, Z. T., Chang-Ming Fang, B. L., Zhao, B., et al. (2011). Using Hyperspectral Vegetation Indices as a Proxy to Monitor Soil Salinity. *Ecol. Indic.* 11, 1552–1562. doi:10.1016/j.ecolind.2011.03.025

Copyright © 2026 Tierra, Castañeda, Gracia and Medina. This is an open-access article distributed under the terms of the Creative Commons Attribution License (CC BY). The use, distribution or reproduction in other forums is permitted, provided the original author(s) and the copyright owner(s) are credited and that the original publication in this journal is cited, in accordance with accepted academic practice. No use, distribution or reproduction is permitted which does not comply with these terms.